

자기터널접합에서 자기 및 자기저항의 접합크기 의존성

상카라나라얀 · 호영강 · 김철기[†] · 김종오 · 이의복

*충남대학교 공과대학 재료공학과
**물리연구소 전기재료부, 인도
***공주대학교 사범대학 물리학과

Junction Size Dependence of Magnetic and Magnetotransport Properties in MTJs

V. K. Sankaranarayanan^{***}, Yongkang Hu^{*}, CheolGi Kim^{*†}, Chong-Oh Kim^{*} and Heebok Lee^{***}

^{*}Department of Materials Science and Engineering, Chungnam National University, Daejeon, 305-764, Korea

^{**}Microstructure Devices Group, Science and Electronic Materials Division, National Physical Laboratory,
Dr. K.S.Krishnan Marg, New Delhi-110012, India

^{***}Department of Physics Education, Kongju National University, Kongju, 314-701, Korea

(2003년 5월 10일 받음, 2003년 6월 13일 최종수정본 받음)

Abstract Magneto-optic Kerr Effect(MOKE), AFM and magnetoresistance measurements have been carried out on as-deposited and annealed Magnetic Tunnel Junctions(MTJs) with junction sizes 180, 250, 320 and 380 μm in order to investigate the correlation among interlayer exchange coupling, surface roughness and junction size. Relatively irregular variations of coercivity H_c (~ 17.5 Oe) and interlayer exchange coupling H_E (~ 7.5 Oe) are observed over the junction in as-deposited sample prepared by DC magnetron sputtering. After annealing at 200°C, H_c decreases to 15 Oe, while H_E increases to 20 Oe with smooth local variation. H_E shows very good correlation with surface roughness across the junction in agreement with Néel's orange peel coupling. The increasing slope per μm of normalized H_c and H_E are same near junction edge along free-layer direction irrespective of junction size, giving relatively uniform H_c and H_E for wider junction size. Thickness profiles of the junctions measured with α -step show increasingly flat top surface for larger junctions, indicating better uniformity for larger junctions in agreement with the normalized H_c and H_E curves. TMR ratios also increase with increasing junction size, indicating improvement for larger uniform junctions.

Key words Coercivity, Exchange coupling, MTJ, Size effect

1. Introduction

Magnetic tunnel junctions(MTJs) exhibiting large tunneling magnetoresistance(TMR) are promising nanostructures for magnetic random access memories (MRAMs).¹⁾ Enormous amount of research has been carried out on TMR materials ever since the first reports of TMR at RT in 1995^{2,3)} and MTJ based MRAMs are on the verge of technological realization. In a spin valve type MTJ, an interfacial coupling at the AFM/FM interface and an interlayer coupling between pinned layer and free layers through the insulating Al-O layer are observed. While the interfacial coupling is important for the stability of the spin valve structure, the interlayer coupling becomes significant in the operational range of MRAMs at low fields and manifests itself as a shift of the minor MR loop. Therefore, a better understanding of the latter over the patterned

junctions assumes added significance. However, magnetic, microstructural and magnetotransport studies are usually reported for the multilayer(ML) films as a whole and not for the micrometer sized patterned junctions. The size and shape of the junctions modify properties,⁴⁾ and localized properties at the junction eventually determine the device stability and performance, irrespective of the properties attained in the initial film and hence such studies are extremely important for devices.

The dominant interlayer coupling in an MTJ with insulating Al-O layer, which prevents electron itinerancy, has been widely accepted to be Néel's orange peel coupling from magnetic dipole interaction related to interfacial morphological corrugations.⁵⁻⁷⁾ The coupling as shown by the proposed relationship⁸⁾ being a sensitive function of the localized properties at the junction, such as surface roughness and thickness distribution over the junction, investigation of various magnetic and magneto-

[†]E-Mail : cgkim@cnu.ac.kr

transport properties over the junction is all the more relevant. Therefore in this study, local M-H loops have been measured on the free layer of magnetic tunnel junctions of different sizes, 180, 250, 320 and 380 μm using a magneto-optic Kerr effect (MOKE) system with 2 μm spatial resolution, and attempted its correlation with the surface roughness estimated from AFM observations.

2. Experimental

Tunnel junctions with the structure, Ta(50 Å)/Cu(100 Å)/Ta(50 Å)/Ni-Fe(20 Å)/Cu(50 Å)/Mn₇₅Ir₂₅(100 Å)/Co₇₀Fe₃₀(25 Å)/Al-O/Co₇₀Fe₃₀(25 Å)/Ni-Fe(600 Å)/Ta(50 Å) were prepared on thermally oxidized Si wafers using DC magnetron sputtering with ultra clean Ar (9N) as a process gas, in a chamber with a base pressure of 3×10^{-9} Torr. The deposition rate were different for different stacks, that is, IrMn of 1.16 Å/sec, Cu of 2.03 Å/sec, Al of 0.37 Å/sec, Ta of 0.915 Å/sec, CoFe of 0.53 Å/sec, NiFe of 0.99 Å/sec. For barrier formation, a 15 Å thick metallic Al film was deposited and subsequently oxidized in an oxidation chamber with a radial line slot antenna (RLSA) for 2.45-GHz microwaves.⁹⁾ Kr was used as the inert gas mixed with O₂ molecular gas for the plasma oxidation. Magnetic field of 30 Oe was applied during deposition.

In-situ patterned junctions were prepared using a shadow mask during deposition, the size of which were 180×180, 250×250, 320×320, and 380×380 μm^2 . The junction samples were thermally annealed at 200°C for 1 hour under a magnetic field of 1 kOe, followed by field cooling. The magneto-optical Kerr effect (MOKE) method was used to obtain the local M-H loops under a 50 Hz driving field. The penetration depth using He-Ne laser light was about 30 nm, which was enough to affect the whole thickness of the free layer. The laser beam size was about 2 μm diameter, corresponding to the spatial resolution of the micro-MOKE system. The field was applied in the annealing field direction. The sample was scanned by using a computer-controlled x-y stage to obtain a two-dimensional plot of magnetic parameters. The scan distances were, respectively, 300 μm along both x-, y-axes for 180×180 and 250×250 μm^2 junctions, and 400 μm along both x-, y-axes for 320×320 μm^2 and 380×380 μm^2 junctions, where the origin of coordinate was regarded as junction center.

MOKE minor loops and Tunneling magnetoresistance (TMR) measurements were carried out on as-deposited and annealed samples. Atomic Force Microscopy (AFM) and α -step thickness profiles were also performed on as-deposited samples with different junction sizes.

3. Results and Discussion

The MOKE hysteresis loops were measured at several points over the junction for the sample annealed at 200°C. M-H loops were measured under a cyclic field along the annealing field direction. There is no shift of the loop at the outside edge of the junction. The shift due to the interlayer exchange coupling field H_E increases as the measuring point moves to the junction center, then decreases as the point moves away from the center. Even though there are local variations in both H_E and H_c , the squareness ratio of the loops is nearly equal to one, except for the loops caused by demagnetizing effects when the measuring point is less than about 10 μm distant from the edge of the junction.

The variation of H_E and H_c for an annealed sample is compared with that for an as-deposited one in Fig. 1(a) and Fig. 1(b) respectively.

As seen in Fig. 1(a), the interlayer exchange coupling H_E , measured from the zero field shift of minor MOKE loop, increases gradually from junction edge, reaches a maximum of about 7.5 Oe at the junction centre and then falls off gradually as we approach the other edge, in the as-deposited sample. After annealing, the relatively irregular variation in the as-deposited sample smoothes out and

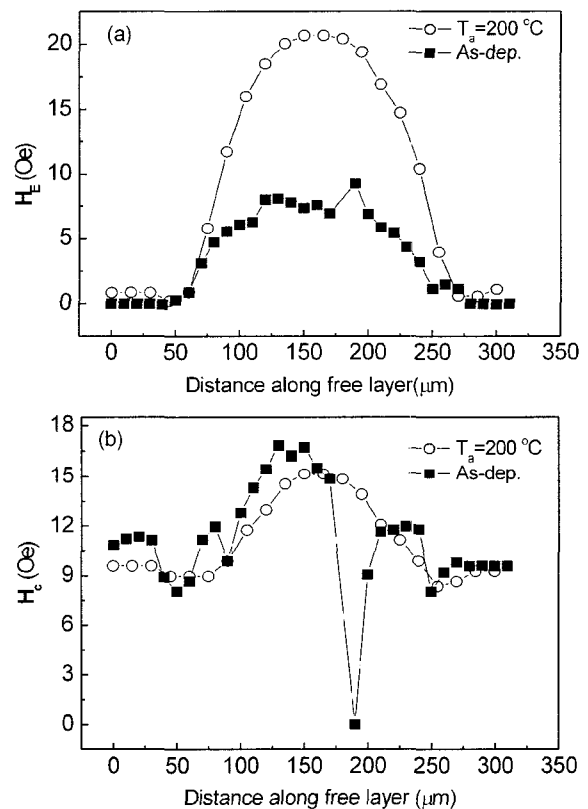


Fig. 1. Variation of interlayer coupling (a) and coercivity (b) over the junction for the as-deposited and annealed MTJs.

increases from 5 Oe at the edge to show a maximum of 20 Oe at the junction centre.

Coercivity H_c also shows similar variation over the junction as given in Fig. 1(b). The H_c in the as-deposited sample is about 10 Oe outside the junction, and a maximum of 17.5 Oe at the junction center. The local variation is quite irregular, with changes of 5 Oe. Annealing leads to smooth variation in H_c over the junction as in the case of H_E . H_c decreases with annealing temperature up to 250°C, and is nearly constant above this temperature

AFM images at several measuring points along the free layer across the junction are shown in Figs. 2(a)-(d). On the free layer outside the junction (point p1), RMS roughness is 3.3 Å, and becomes smaller, 2.3 Å, near the edge of the junction (p2). The roughness increases to 5.8 Å as the measuring point moves to the center of the junction (p3), and then decreases as the point moves to the other edge (p4). The variation of RMS surface roughness across the junction is shown in Fig. 3.

The interlayer coupling in the tunnel junction sample with insulating spacer layers is more likely to be Néel's orange peel coupling than RKKY type. In the proposed relationship for orange peel coupling,⁸ the surface roughness 'h' has a square term in the numerator and hence the coupling could be expected to be about 4 to 5 times larger than that near the edge. It may be noticed in Fig. 3 that the RMS surface roughness measured over the junction in AFM measurements increases from 2.5 Å near the edge to

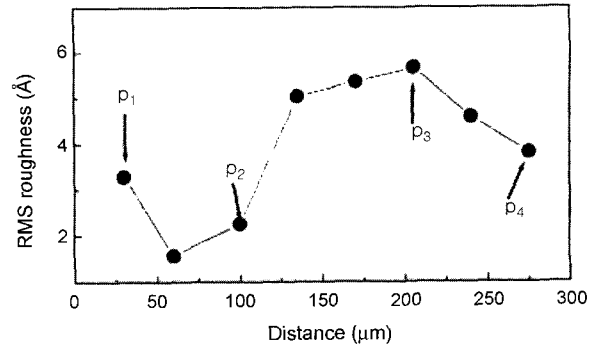


Fig. 3. RMS surface roughness variation over the junction for an as-deposited MTJ.

5.5 Å at the junction center. Remarkably, the observed interlayer coupling at the junction centre (20 Oe given above), agrees well with this expected value. It also confirms the validity of the Néel's coupling in the present case.

Figures 4(a) and (b), respectively show the variation of normalized H_c and H_E values for annealed samples for different junction sizes. There is a gradual increase in the normalized H_c on moving from the edge towards the center, where the value at edge is 0.6 for $180 \times 180 \mu\text{m}^2$ sample, but is 0.4 for other samples. That is, H_c of 8.5 Oe at edge increases to 15 Oe at junction center for sample of $180 \mu\text{m}$, as shown in the inset of Fig. 4(a), and H_c of 6 Oe at edge increases to 17 Oe for other samples. The increasing slope of normalized H_c is same near the edge

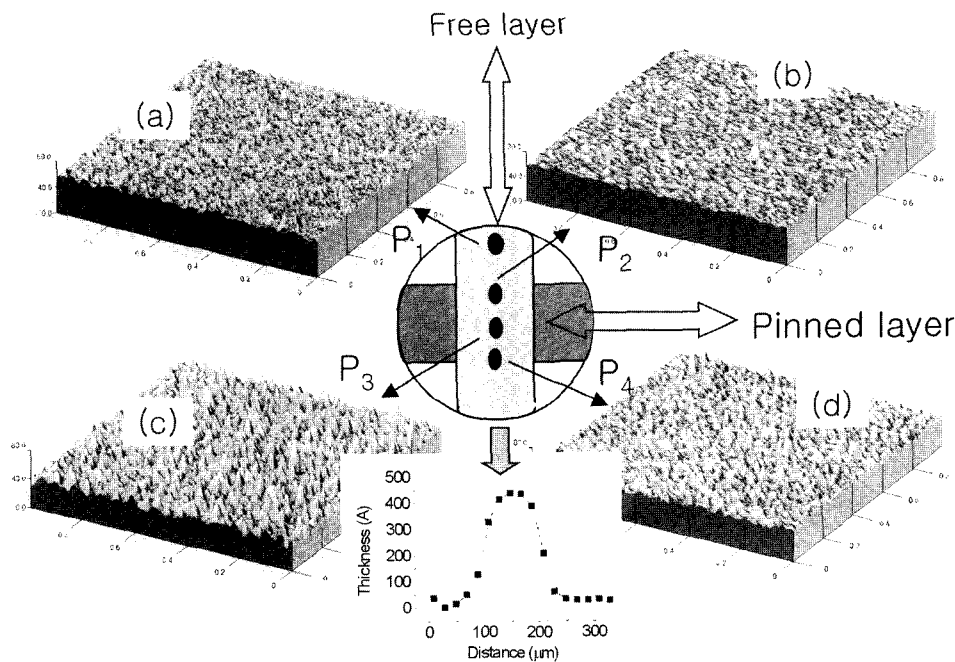


Fig. 2. AFM images along the free layer across the junction, (a) at point p1 (R_{RMS} : 3.3 Å), outside the layer, (b) point p2 (R_{RMS} : 2.3 Å), near left edge, (c) point p3 (R_{RMS} : 5.8 Å), junction center, and (d) point p4 (R_{RMS} : 2.5 Å), near right edge. (scan area: $1 \times 1 \mu\text{m}^2$). Inset figure shows the variation of film thickness across the junction center, checked by α -stepper.

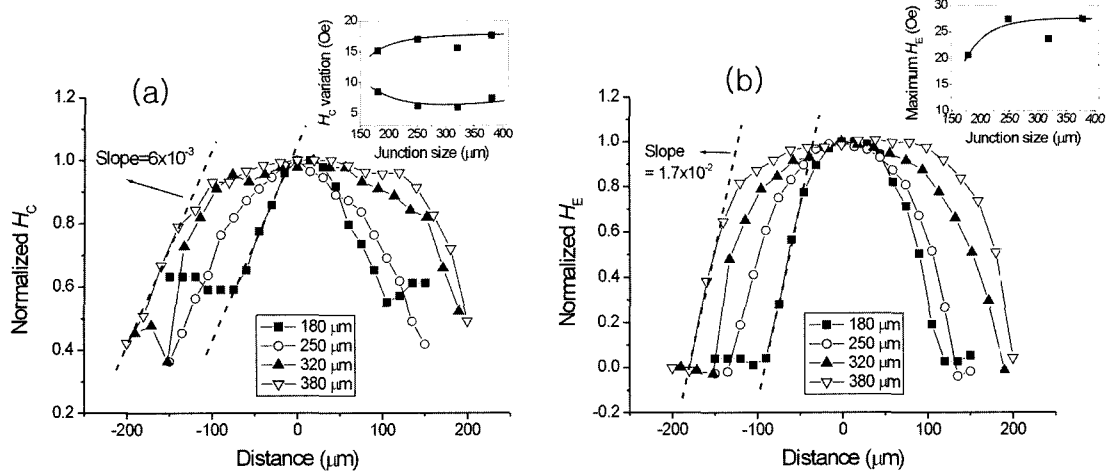


Fig. 4. Variation of normalized H_c and H_E for different junction sizes over the junction. The insets show the variation of H_c and maximum H_E values for junctions with different sizes.

for all samples as marked by broken lines in Fig. 4(a), in which the slope for variation of normalized H_c per μm is 6×10^{-3} . The normalized H_E also reveals same increasing rate near edge for all samples as depicted in broken lines of Fig. 4(b), and its variation slope per μm is 1.7×10^{-2} . Here, the maximum H_E at junction center increases from 20 to 27 Oe with junction size, as shown in inset of Fig. 4(b). Even though it is hard to attribute this edge effect to variations in multilayer stack parameters resulting from angular distribution of sputtered beam intensity,¹⁰ these gradual changes of H_c and H_E near the edge may be due to the gradual change of stack's thickness and surface roughness.

Normalized values of H_E and H_c show gradual increase from the edge with similar slopes for different junction sizes near the edge of the junction. Increasingly flatter top in these curves with increasing junction size indicate constancy of the H_E and H_c values over the junction in larger junctions.

Fig. 5 shows the gradual change of film thickness over the junction for junctions with different size, measured by an α -stepper. This variation may arise from edge effects of in-situ mask patterning with the angular distribution of sputtered beam intensity.¹⁰ Thickness profiles of the junctions reveal flat tops for larger junctions as shown in Fig. 5. The profile for the junction with a smaller size has a curved top. As the junction size increases the top surface becomes increasingly flatter and the largest junction has a very flat top surface. It is a clear indication of better uniformity over the junction with increasing size, which is also reflected in the normalized H_E and H_c curves, as shown earlier.

TMR ratios and minor loop width ΔH are plotted as a function of junction size in Fig. 6. The inset shows the

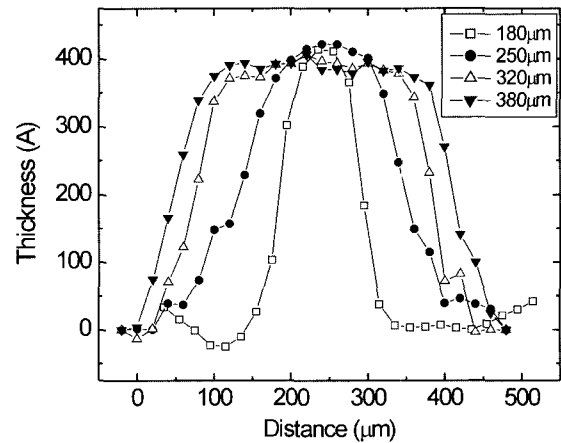


Fig. 5. α -step thickness variation over the junctions

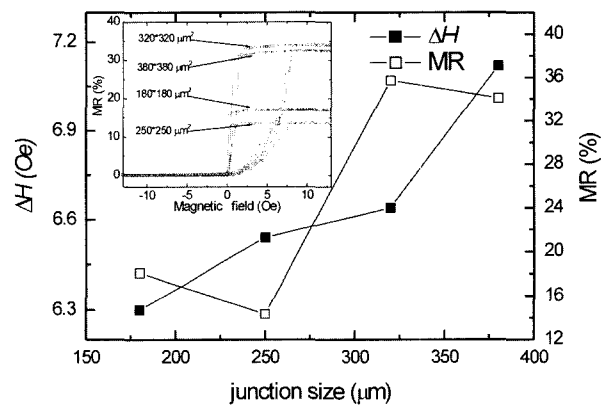


Fig. 6. Variation of MR ratio and ΔH as a function of junction size; Inset shows the minor MR loops.

TMR minor loops for these junctions. We observed TMR ratios up to 36% at room temperature for the junctions oxidized for 10 seconds. Higher oxidation times of 13 and 16 seconds lead to decrease in TMR ratios. After an initial fall, the TMR ratios increase on increasing junction size

from 250 to 320 μm for both as-deposited and annealed samples and starts decreasing for still larger size as shown in the Figure. The improvement with junction size could be due to better uniformity. The small ups and downs in TMR ratios are within the fluctuation limits of TMR that is usually observed even among junctions fabricated in the same batch. The widths of the TMR minor loops, ΔH , as seen in Fig., increase with increasing junction size. A similar increase of ΔH with increasing junction size was observed for higher oxidation times also, though the TMR ratios were relatively lower. Since half of ΔH would correspond to the coercivity H_c , the increase of ΔH values could mean an increase in coercivity. A qualitatively similar variation of coercivity with junction size was observed in MOKE measurements.

4. Conclusions

Local M-H loops have been measured on the free layer of multilayer magnetic tunnel junctions (MTJ), and the variations have been compared with local variation of RMS surface roughness, thickness and pattern size. Relatively irregular variations of coercivity H_c (~ 17.5 Oe) and exchange coupling H_E (~ 7.5 Oe) are observed in as-deposited samples, whereas in annealed films, H_c decreases to 15 Oe, and H_E increases to 20 Oe, with smooth local variation over the junction. The magnetic tunnel junctions show h^2 correlation of interlayer exchange coupling H_E with surface roughness, in agreement with the expected Néel's orange peel coupling. The normalised H_E and H_c values show similar slopes at junction edges for different junction sizes and flatter top surface for larger junctions. The local H_c and H_E variations may be a geometric effect of the deposition process using a shadow mask. The α -step

thickness profiles show increasingly flatter top for larger junction sizes, indicating better uniformity over the junction with increasing size, in agreement with the normalized H_E and H_c curves. Improved MR ratios are observed with increasing junction sizes due to better uniformity in larger junctions, in agreement with the observations for normalized H_E and H_c values and thickness profiles.

Acknowledgements

This work was supported by Chungnam National University in program year 2001. Dr. V.K. Sankaranarayanan acknowledges the Brainpool Program for financial support.

References

1. S. S. P. Parkin, K. P. Roche, M. G. Samant, P. M. Rice, R. B. Beyers, R. E. Scheuerlein, E. J. O'Sullivan, S. L. Brown, J. Bucchigano, D. W. Abraham, Yu Lu, M. Rooks, P. L. Trouilloud, R. A. Wanner and W. J. Gallagher, *J. Appl. Phys.*, **85**, 5828 (1999).
2. J. S. Moodera, L. R. Kinder, T. M. Wong and R. Meservey, *Phys. Rev. Lett.*, **74**, 3273 (1995)
3. T. Miyazaki and N. Tezuka, *J. Magn. Magn. Mater.*, **139**, L231 (1995)
4. C. G. Kim, T. Shoyama, M. Tsunoda, M. Takahashi, T. Y. Lee and C. O. Kim *Korean J. Magnetics*, **7**, 72 (2002).
5. M. Julliere, *Phys. Lett.*, **54A**, 225 (1975).
6. J. C. Slonczewski, *Phys. Rev.*, **B39**, 6995 (1989).
7. J. S. Moodera, L. R. Kinder, J. Nowak, P. LeClair and R. Meservey, *Appl. Phys. Lett.*, **69**, 708 (1996).
8. J. C. S. Cools, W. Kula, D. Mauri and T. Lin *J. Appl. Phys.*, **85**, 4466 (1999).
9. M. Tsunoda, K. Nishigawa, S. Ogata, M. Takahashi, *Appl. Phys. Lett.*, **80** (2002) 3135.
10. J. E. Mahan, *Physical vapor deposition of thin films*, A Wiley-Interscience Publication, 2000, Ch. VII.5.